Journal of proteome research

Article

pubs.acs.org/jpr

Proteome Profiling and Ultrastructural Characterization of the Human RCMH Cell Line: Myoblastic Properties and Suitability for Myopathological Studies

Laxmikanth Kollipara,[†] Stephan Buchkremer,[‡] Joachim Weis,[‡] Eva Brauers,[‡] Mareike Hoss,[§] Stephan Rütten,[§] Pablo Caviedes,[∥] René P. Zahedi,[†] and Andreas Roos*[,†,‡]

[†]Leibniz-Institut für Analytische Wissenschaften, ISAS e.V., Otto-Hahn-Str. 6b, 44227 Dortmund, Germany

[‡]Institute of Neuropathology, RWTH Aachen University Hospital, Pauwelsstrasse 30, D-52074 Aachen, Germany

[§]Electron Microscopic Facility, Institute of Pathology, RWTH Aachen University Hospital, D-52074 Aachen, Germany

[∥]Programa de Farmacología Molecular y Clínica, ICBM, Facultad de Medicina, Universidad de Chile, Santiago 1058, Chile

Supporting Information

ABSTRACT: Studying (neuro)muscular disorders is a major topic in biomedicine with a demand for suitable model systems. Continuous cell culture (in vitro) systems have several technical advantages over in vivo systems and became widely used tools for discovering physiological/pathophysiological mechanisms in muscle. In particular, myoblast cell lines are suitable model systems to study complex biochemical adaptations occurring in skeletal muscle and cellular responses to altered genetic/environmental conditions. Whereas most in vitro studies use extensively characterized murine C_2C_{12} cells, a comprehensive description of an equivalent human cell line, not genetically manipulated for immortalization, is lacking. Therefore, we characterized human immortal myoblastic RCMH cells using scanning (SEM) and transmission electron microscopy (TEM) and proteomics. Among more than 6200 identified proteins we confirm the known expression of proteins important for muscle function. Comparing the RCMH proteome with two well-defined nonskeletal muscle cells lines (HeLa, U2OS) revealed a considerable enrichment of proteins important for muscle function. SEM/TEM confirmed the presence of agglomerates of cytoskeletal components/intermediate filaments and a prominent rough ER. In conclusion, our results indicate RMCH as a suitable in vitro model for investigating muscle function-related processes such as mechanical stress burden and mechano-transduction, EC coupling, cytoskeleton, muscle cell metabolism and development, and (ER-associated) myopathic disorders.

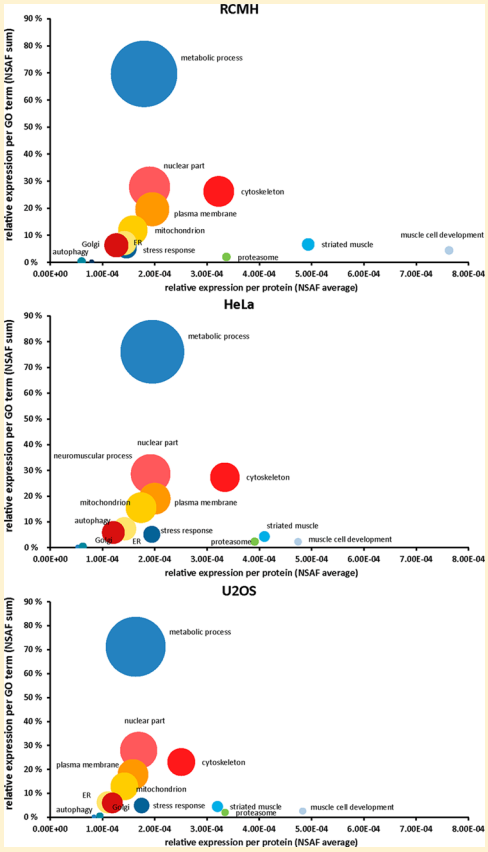

KEYWORDS: *RCMH, myoblasts, human muscle cell line, proteome profiling, muscle proteomics*

INTRODUCTION

Functional, biochemical, and morphological studies using continuous cell culture (in vitro) have a number of advantages over in vivo studies. In general, in vitro systems are easier to handle, and therefore technical but even more important biological variability is considerably reduced, improving reproducibility while allowing us to conduct experiments under well-defined conditions without limitations of sample material.[1] Therefore, in vitro studies have become common and useful tools either for studying physiological and pathophysiological mechanisms or for proof-of-principle examinations evaluating a potential use in myogenic stem-cell-based therapy.[2] Undifferentiated myoblast cell lines serve as model systems for

Received: October 19, 2015
Published: January 19, 2016

DOI: 10.1021/acs.jproteome.5b00972
J. Proteome Res. 2016, 15, 945−955

investigating the complex biochemical adaptations occurring in skeletal muscle under different conditions.[3−7] Moreover, cellular responses to altered genetic or environmental conditions can be studied to obtain deeper insights into the pathophysiology of myopathic disorders.[8,9] Human inherited and acquired myopathies are in the focus of current research. A wide range of respective in vitro studies were performed using C_2C_{12} cells, a well-defined and extensively characterized murine myoblastic cell line.[3−7,10] Apart from that, a growing number of human immortalized myoblast cell lines, generated by human telomerase reverse transcriptase overexpression (hTERT immortalization), were studied and characterized also using proteomics;[11−14] however, a comprehensive description for an equivalent cell line of human origin, immortalized without genetic manipulation, is lacking. In this context, knowledge of the underlying cellular characteristics on both the morphological and the biochemical level is decisive for well-planned hypothesis-driven studies. To fill this gap of knowledge, we characterized the human myoblastic cell line RCMH.[15,16] The human spontaneously immortalized adherent RCMH myoblastic cell line was established by Caviedes and Freeman in 1992.[15] (For further information and use of this cell line, please contact Dr. Pablo Caviedes, pcaviede@med.uchile.cl.) Since then, expression of the cytoskeletal proteins α-actinin, α-sarcomeric actin, myosin, titin, vimentin, desmin, the muscle specific myoglobin, creatine kinase, and dystrophin as well as presence of receptors for α-bungarotoxin, dihydropyridine, ryanodine, and an active IP3 metabolism have been reported.[15−18]

Here we combined proteome profiling to investigate the molecular composition of RCMH cells[19] with scanning (SEM) and transmission electron microscopy (TEM) focusing on morphological characteristics. We identified 6236 unique proteins spanning approximately 5 orders of magnitude in protein abundance. Electron microscopic (EM) studies revealed the presence of microvilli on the cell surface as well as prominent endoplasmic reticulum (ER) networks. This study expands our knowledge on human RCMH myoblast morphology and protein composition and confirms that this cell line is a suitable in vitro system to study muscle physiology and pathology, especially with regard to ER-related processes and other cellular mechanisms altered in myopathy.

EXPERIMENTAL PROCEDURES

Culturing of RCMH Cells

After defrosting RCMH cells were cultured in Dulbecco's modified Eagle's medium F-12-Ham containing 0.1% sodium bicarbonate (Sigma-Aldrich, Taufkirchen, Germany) and 12.5% fetal calf serum (Biowest) at 37 °C in a 5% CO_2 atmosphere to a confluence of ∼70% before being subjected to morphological and proteomic studies.

Sample Processing for Electron Microscopic Studies

For transmission electron microscopic studies, RCMH cells grown in culture dishes were gently scraped, centrifuged at 500*g*, and washed with 1× PBS (room temperature). Subsequently, cells were fixed with 2.5% glutaraldehyde in 0.1 M phosphate buffer for 12 h. Pellets were further processed and samples were analyzed as previously reported.[20] For scanning electron microscopic studies, RCMH cells were fixed in 3.0% glutaraldehyde in 0.1 M phosphate buffer for at least 4 h at room temperature, rinsed with sodium phosphate buffer (0.1 M, pH 7.39, Merck, Darmstadt, Germany), and dehydrated by incubating consecutively in ascending ethanol series (30, 50, 70, and 90%) with a final incubation in 100% ethanol for 10 min. The latter was repeated three times. Cells were incubated for 20 min in hexamethyldisilaxane (Sigma-Aldrich, Steinheim, Germany) and air-dried. After fixation on a section table, samples were sputter-coated (Leica EMS CD 500) with a 10 nm gold layer. Samples were analyzed using an environmental scanning electron microscope (ESEM XL 30 FEG, FEI, Eindhoven, The Netherlands) in a high vacuum environment using an acceleration voltage of 10 kV.

Sample Preparation for Proteomics Analysis

Cell Lysis and Protein Extraction. Approximately 2 mg of cells was lysed using 0.5 mL of 50 mM Tris-HCl (pH 7.8) buffer containing 150 mM NaCl, 1% sodium dodecyl sulfate (SDS), and complete mini-EDTA free. Subsequently, 6 μL of benzonase (25 U/μL) and 2 mM $MgCl_2$ were added to the lysate and incubated at 37 °C for 30 min. The cell lysate was clarified by centrifugation at 20 000 rcf and 4 °C for 30 min. To the supernatant, ice cold ethanol was added in 10-fold excess and stored at −40 °C for 1 h followed by centrifugation as above. The pellet was washed with 200 μL of ice cold acetone and was allowed to dry under laminar flow hood.

Protein Digestion and Reversed-Phase (RP) Peptide Fractionation at pH 6.0. The protein pellet was resolubilized with 0.3 mL of 6 M GuHCL/50 mM NH_4HCO_3 buffer (pH 7.8), and protein concentration was determined by BCA assay according to the manufacturer's instructions (Pierce BCA Protein Assay Kit, Thermo Scientific). Cysteines were reduced with 10 mM dithiothreitol (DTT) at 56 °C for 30 min, and the free thiols were carbamidomethylated with 30 mM iodoacetamide (IAA) at RT for 30 min in the dark. Sample cleaning and enzymatic proteolysis were carried out based on the filter-aided sample preparation (FASP) protocol.[21,22] An aliquot corresponding to 100 μg of protein was diluted 2-fold with 50 mM ammonium bicarbonate (NH_4HCO_3) buffer (pH 7.8) and loaded on a 30 kDa molecular weight cutoff (MWCO) membrane filer (Microcon), which was centrifuged at 13 900 rcf for 30 min. The filter was washed thrice with 100 μL of 50 mM NH_4HCO_3 buffer (pH 7.8) by centrifugation at 13 900 rcf for 15 min each. Finally, 100 μL of digestion buffer comprising 2.5 μg of trypsin (Promega), in 0.2 M GuHCl, 2 mM $CaCl_2$, and 50 mM NH_4HCO_3 buffer (pH 7.8), was added and incubated overnight at 37 °C. The generated tryptic peptides were recovered by centrifugation with 50 μL of 50 mM NH_4HCO_3, followed by 50 μL of ultrapure water. Finally, the peptides were acidified to pH ∼3 using 10% TFA (v/v). Proteolytic digests were quality-controlled, as previously described.[23] Acidified peptides were desalted with C18 solid-phase extraction cartridges (SPEC, 4 mg, Varian) according to the manufacturer's instructions, and the eluted peptides were dried under vacuum. The dried peptide pellet was resuspended in buffer A (10 mM ammonium acetate, pH 6.0), and an aliquot equivalent to 25 μg was fractionated on an Ultimate 3000 LC system (Thermo Scientific) using reversed-phase chromatography at pH 6.0. Peptides were separated on a 1 mm × 150 mm C18 (ZORBAX 300SB) column with a 75 min LC gradient ranging from 3 to 50% buffer B (84% ACN in 10 mM ammonium acetate, pH 6.0) at a flow rate of 12.5 μL/min. In total, 16 fractions were collected at 1 min intervals in concatenated manner. Each fraction was dried under vacuum and resuspended in 15 μL of 0.1% TFA for nano-LC−MS/MS analysis.

DOI: 10.1021/acs.jproteome.5b00972
J. Proteome Res. 2016, 15, 945−955

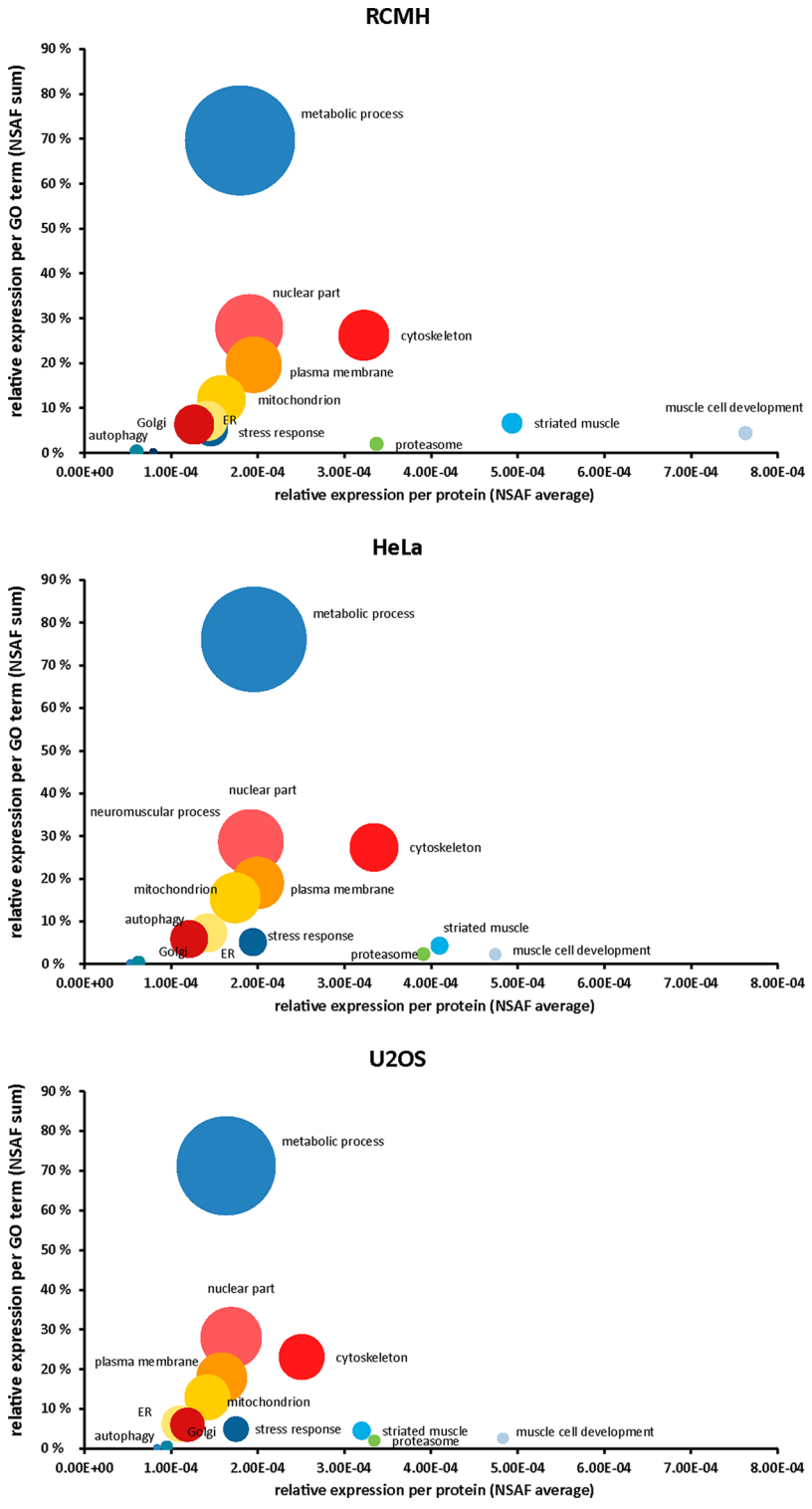

Figure 1. Comparison of proteomic data from RCMH, HeLa, and U2OS cells. All three data sets were searched and processed in the same way, and NSAF (normalized spectral abundance factor) values for 6244 (RCMH), 6304 (HeLa), and 7158 (U2OS) proteins were determined as a measure of normalized protein abundance in the respective cell type. For selected GO terms the following parameters were determined: (i) the number of proteins corresponding to this GO term, represented by size of the bubbles, and (ii) the sum of the individual NSAF values of these proteins, represented as the share of the complete proteome on the *Y* axis. This value reflects the relative expression of the particular GO term; for example, ~6.6% of the protein molecules detected in RCMH are related to the GO term "striated muscle", compared with 4.3% for HeLa and 4.5% for U2OS (see also Table 1). (iii) The average NSAF per protein of the respective GO term, reflecting the relative expression per protein. Processes important for studying muscle cell function (neuromuscular process, muscle cell development, striated muscle) are overrepresented in the RCMH cells, as compared with U2OS and HeLa.

Nano-LC–MS/MS Analysis. All 16 fractions were analyzed using an Ultimate 3000 nano RSLC system coupled to an Orbitrap Elite mass spectrometer (both Thermo Scientific). Peptides were preconcentrated on a 75 μm × 2 cm C18

DOI: 10.1021/acs.jproteome.5b00972
J. Proteome Res. 2016, 15, 945–955

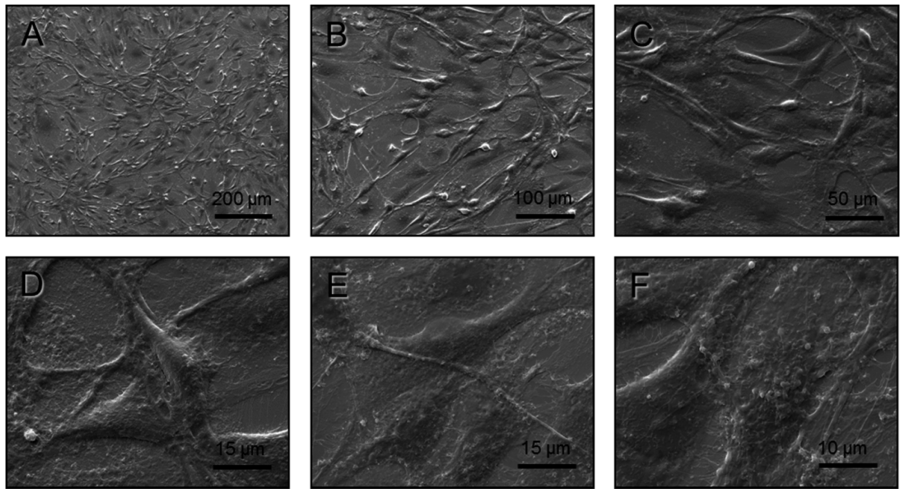

Figure 2. Morphological surface studies of RCMH cells using SEM: (A−C) Spread elongated cells (diameter: ∼10 μm) forming a network. Studies indicate numerous cytoplasmic extensions on the surface of these cells (D−F).

trapping column for 10 min using 0.1% TFA (v/v) with a flow rate of 20 μL/min, followed by separation on a 75 μm × 50 cm C18 main column (both Pepmap, Thermo Scientific) with a 128 min LC gradient ranging from 3 to 42% B (84% ACN in 0.1% FA) at a flow rate of 250 nL/min. MS survey scans were acquired in the Orbitrap from 300 to 1500 m/z at a resolution of 60 000 using the polysiloxane ion at 371.101236 m/z as lock mass.[24] The 15 most intense ions were subjected to collision-induced dissociation (CID) in the ion trap, taking into account a dynamic exclusion of 30 s. CID spectra were acquired with a normalized collision energy of 35% and an activation time of 10 ms. AGC target values were set to 10^6 for Orbitrap MS and 10^4 for ion trap MS^n scans, and maximum injection times were set to 100 ms for both full MS and MS^n scans.

MS Data Analysis. MS raw data were converted into peak lists (mgf files) using the ProteoWizard software (version 2.2.2954)[25] and were searched against a concatenated target/decoy version of the human Uniprot database (downloaded on 11th of December 2013, containing 20 273 target sequences) using Mascot 2.4 (Matrix Science), MS-GF+,[26,27] and X! Tandem Jackhammer (2013.06.15) with the help of searchGUI 1.18.4.[28] Trypsin with a maximum of two missed cleavages was selected as enzyme. Carbamidomethylation of Cys was set as fixed, and oxidation of Met was selected as variable modification. MS and MS/MS tolerances were set to 10 ppm and 0.5 Da, respectively. The results of the different search algorithms were imported into the PeptideShaker software 0.29.1[29] for thresholding the data using a false discovery rate (FDR) of 1% on the PSM, peptide, and protein level. The quality-controlled data was exported, and only proteins that were identified with ≥1 validated peptide were considered for data analysis. NSAF (normalized spectral abundance factor)[30] values were calculated, and additional information like subcellular location and disease, was retrieved from the Uniprot Web site (http://www.uniprot.org/) to roughly estimate the abundance of the identified proteins.

The mass spectrometry proteomics data have been deposited to the ProteomeXchange Consortium[31] via the PRIDE partner repository with the data set identifier PXD001974 and 10.6019/PXD001974.

RESULTS

The comprehensive characterization of a cell line is a mandatory step to classify its suitability for (i) studying physiological processes, (ii) discovering pathological processes, and (iii) developing novel cell-based therapies for human genetic diseases, including muscular disorders.[9,32] Mass-spectrometry-based proteome profiling provides unique and broad insights into protein composition and allows a general understanding of biological systems.[19,33] Here we analyzed the morphological characteristics and the proteome of the human immortal RCMH myoblastic cell line. We identified 6244 proteins (Supplemental Table 1) with a false discovery rate (FDR) of ≤1% on the peptide spectrum match, peptide, and protein level. Determined NSAF values, which correlate to the relative expression of a protein within the respective cell line, cover a range of more than four orders of magnitude between the most abundant protein actin (ACTG1) and the ryanodine receptor 3 (RYR3). According to Uniprot KB and considering multiple subcellular localizations, 2132 proteins are localized in the cytoplasm (398 cytoskeletal), 1957 in the nucleus, 500 in mitochondria, 355 in the ER, 264 in the Golgi and 69 in lysosomes, whereas 169 proteins are secreted. To classify the composition of the RCMH proteome, we analyzed all 6236 identified proteins for an enrichment of GO (gene ontology) terms compared with the human proteome. Indeed, this analysis did not show major differences between RCMH and other cell types. We hypothesize that this might be a consequence of the undifferentiated stage of the RCMH cell line in the culture conditions utilized, which favor proliferation rather than fusion and myotube formation in vitro[34] or the general way of GO term analysis, which merely takes into account proteins, rather than their expression levels. Consequently, as long as similar numbers of proteins for a given GO term are detected in two different cell types, they produce similar results, even if the respective proteins are considerably higher expressed in one of the two cell types. Therefore, we decided to look for a subset of GO terms that with respect to the origin of these cells play a role in muscle function or are involved in myopathic disorders. For the corresponding proteins we determined their relative abundances by considering their NSAF values as a measure of protein expression. Additionally, the individual abundance of each protein was

DOI: 10.1021/acs.jproteome.5b00972
J. Proteome Res. 2016, 15, 945−955

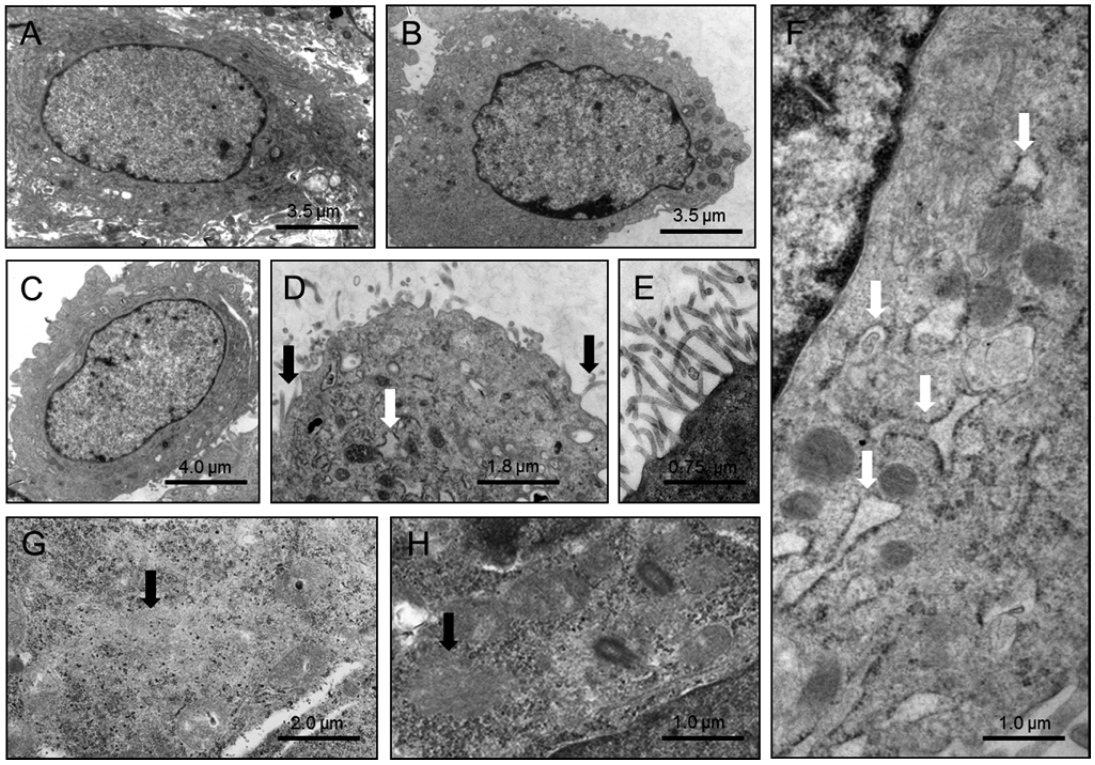

Figure 3. Morphological studies of RCMH cells using TEM: (A–C) Large (myo)nuclei (diameter: ∼5 μm) with peripheral condensed chromatin. (D,E) Cytoplasmic extensions on the cell surface (length: ∼1 μm) indicated black arrows and (D,F) prominent (sarco)endoplasmic reticulum indicated by white arrows. (G,H) Black arrows indicate accumulations of cytoskeletal components/intermediate filaments.

compared with the abundance of GAPDH, a well-known house-keeping protein. Next, we compared the obtained values with two other cell types with well-characterized proteomes, namely, HeLa and U2OS cells, to identify an up/down-regulation of certain pathways and biological functions in RCMH cells. Comprehensive raw data of hTERT immortalized myoblastic cells derived from healthy donors were not available for our comparison. We researched the raw data from Guo et al. (HeLa)[35] and Beck et al. (U2OS)[36] using the same software and settings as applied to our own RCMH data. This led to the identification of 6304 (89 groups) HeLa and 7158 (84 groups) U2OS proteins (with at least 1 validated peptide) compared with the 6244 (111 groups) proteins in RCMH. Next, for the following GO terms we extracted NSAF values of the corresponding proteins in each sample: cytoskeleton (GO:0005856), proteasome complex (GO:0000502), striated muscle (combination of adaptation (GO:0014888), atrophy (GO:0014891), cell development (GO:0055002), nuclear part (GO:0044428), plasma membrane (GO:0005886), mitochondrion (GO:0005739), regulation of response to stress (GO:0080134), muscle cell development (GO:0055001), metabolic process (GO:0008152), endoplasmic reticulum (GO:0005783), Golgi apparatus (GO:0005794), neuromuscular process (GO:0050905), and autophagy (GO:0006914). For each GO term and sample we (i) determined the number of corresponding proteins and (ii) calculated the sum of the individual protein NSAF values. This represents the relative expression of that GO term within the respective proteome. Moreover, (iii) we calculated the average NSAF value per protein (NSAF sum divided by the number of proteins), which reflects the relative expression per protein of that GO term. These values are presented in Figure 1 as a representative comparison of the different proteomes. Thus, differences in the expression patterns of RCMH, HeLa, and U2OS become apparent: For instance, proteins corresponding to striated muscle are clearly more abundant in RCMH than in U2OS and HeLa. The same holds true for proteins involved in muscle cell development.

Morphological studies of RCMH cells grown for 24 h were performed using transmission (TEM) and scanning (SEM) electron microscopy. SEM studies revealed spread cells that exhibit cytoplasmic extensions (see Figure 2). TEM studies confirmed the presence of cytoplasmic extensions and moreover revealed large nuclei (relative to cytoplasm) and a prominent ribosome dense sarcoendoplasmic reticulum as well as accumulations of cytoskeletal components/intermediate filaments (see Figure 3).

■ DISCUSSION

RCMH Proteome Composition Allows Investigation of Cytoskeleton and Mechanical Stress Burden

Skeletal muscle consists of tightly bundled cylindrical multinucleated cells, each packed with myofibrils, which form the bulk of muscle mass. They are composed of ordered tandem arrays of sarcomeres, the core structural unit of dynamically interacting chains of actin and myosin. Together, these filaments account for nearly 40% of the total mass of the human body and are responsible for muscle contraction.[4] This, in turn, reflects expectations in a suitable cell model for in vitro muscle studies, in which several important cytoskeletal components apart from actin and myosin are expressed, such as desmin and titin. Notably, in RCMH cells desmin is among the 100 most abundant proteins, whereas it could not be detected in the two control cell lines. Moreover, our MS data

DOI: 10.1021/acs.jproteome.5b00972
J. Proteome Res. 2016, 15, 945–955

Table 1. Quantitative GO Term Representation in RCMH, HeLa, and U2OS Cells Shows Differences in Cellular Composition[a]

RCMH			
GO term	relative expression term (sum NSAF)	no. proteins	relative expression per protein (⌀ NSAF)
cytoskeleton (GO:0005856)	26.2%	813	0.032%
proteasome complex (GO:0000502)	2.0%	59	0.034%
striated muscle (adaptation, atrophy, cell development)	6.6%	134	0.049%
nuclear part (GO:0044428)	27.8%	1464	0.019%
plasma membrane (GO:0005886)	19.6%	1005	0.020%
mitochondrion (GO:0005739)	11.9%	752	0.016%
regulation of response to stress (GO:0080134)	5.2%	359	0.015%
muscle cell development (GO:0055001)	4.4%	58	0.076%
metabolic process (GO:0008152)	69.6%	3878	0.018%
endoplasmic reticulum (GO:0005783)	7.1%	504	0.014%
Golgi apparatus (GO:0005794)	6.3%	498	0.013%
neuromuscular process (GO:0050905)	0.2%	19	0.008%
autophagy (GO:0006914)	0.3%	57	0.006%

HeLa			
GO term	relative expression term (sum NSAF)	no. proteins	relative expression per protein (⌀ NSAF)
cytoskeleton (GO:0005856)	27.3%	819	0.033%
proteasome complex (GO:0000502)	2.3%	60	0.039%
striated muscle (adaptation, atrophy, cell development)	4.3%	105	0.041%
nuclear part (GO:0044428)	28.6%	1493	0.019%
plasma membrane (GO:0005886)	19.0%	953	0.020%
mitochondrion (GO:0005739)	15.5%	893	0.017%
regulation of response to stress (GO:0080134)	5.1%	265	0.019%
muscle cell development (GO:0055001)	2.3%	48	0.047%
metabolic process (GO:0008152)	76.1%	3896	0.020%
endoplasmic reticulum (GO:0005783)	7.3%	514	0.014%
Golgi apparatus (GO:0005794)	5.9%	487	0.012%
neuromuscular process (GO:0050905)	0.1%	23	0.005%
autophagy (GO:0006914)	0.4%	58	0.006%

U2OS			
GO term	relative expression term (sum NSAF)	no. proteins	relative expression per protein (⌀ NSAF)
cytoskeleton (GO:0005856)	23.1%	920	0.025%
proteasome complex (GO:0000502)	2.0%	61	0.033%
striated muscle (adaptation, atrophy, cell development)	4.5%	141	0.032%
nuclear part (GO:0044428)	27.9%	1650	0.017%
plasma membrane (GO:0005886)	17.9%	1128	0.016%
mitochondrion (GO:0005739)	12.9%	912	0.014%
regulation of response to stress (GO:0080134)	4.9%	282	0.017%
muscle cell development (GO:0055001)	2.6%	54	0.048%
metabolic process (GO:0008152)	71.2%	4349	0.016%
endoplasmic reticulum (GO:0005783)	6.3%	568	0.011%
Golgi apparatus (GO:0005794)	6.0%	507	0.012%
neuromuscular process (GO:0050905)	0.2%	22	0.008%
autophagy (GO:0006914)	0.6%	59	0.010%

[a]Relative expression per GO term (sum NSAF) and per protein (average NSAF) were calculated for selected GO terms based on the corresponding proteins identified in the respective cell lines.

indicate substantially higher levels of actin and myosin in RCMH cells, compared with HeLa and U2OS (see Supplemental Table 1). In general, proteins belonging to the GO term cytoskeleton (GO:0005856) are more highly expressed in RCMH, both on average and in sum (see Figure 1; Tables 1 and 2). We found a considerable number and expression of cytoskeletal proteins, with a high abundance of beta- and gamma-actin concomitant with expression of different actin-related or processing proteins such as F-actin-capping protein subunits α-1, α-2, β, Rho-associated protein kinase 1 and 2, cofilin-1 and 2, and calponin-2 and 3. Moreover, expression of different myosin light and heavy chains as well as 12 different unconventional myosins, 3 tropomyosins, and a myosin phosphatase Rho interacting protein (MPRIP), serving in intracellular movements, could be demonstrated. Notably, the expression levels of these unconventional myosins were substantially higher than in HeLa (NSAF ~ 5-fold higher) and U2OS cells (NSAF ~1.5-fold higher). The dynamic structure of the cytoskeleton also contributes to cell stability during the contraction cycle by anchoring myofibrils to subcellular compartments via respective linker proteins. In this context, we also identified expression of such linker proteins such as α- and β-chain spectrins (expression levels higher than in HeLa but similar to U2OS) together with calmodulin-regulated spectrin-associated proteins 1 and 2 (likewise). Filamins (connecting the plasma membrane to the cytoskeleton) and respective assembly promoting proteins like α-, β-, and γ-adducin (membrane-cytoskeleton-associated protein that promotes the assembly of the spectrin-actin network; expression considerably higher than in HeLa and similar to U2OS levels) as well as dystrophin (DMD; connecting intracellular cytoskeletal filaments and extracellular matrix; expression substantially higher than in both HeLa and U2OS) were also detected. These proteins are known to stabilize mechano-

DOI: 10.1021/acs.jproteome.5b00972
J. Proteome Res. 2016, 15, 945−955

Table 2. Comparison of GO Term Expression Levels between RCMH, HeLa and U2OS Cells, Based on Both NSAF Sum and NSAF Average

GO Term	sum RCMH/HeLa	average RCMH/HeLa	sum RCMH/U2OS	average RCMH/U2OS
cytoskeleton	0.96	0.97	1.14	1.29
proteasome complex	0.85	0.86	0.97	1.01
striated muscle	1.54	1.21	1.47	1.54
nuclear part	0.97	0.99	0.99	1.12
plasma membrane	1.03	0.98	1.10	1.23
mitochondrion	0.77	0.91	0.92	1.11
regulation of response to stress	1.02	0.75	1.06	0.83
muscle cell development	1.95	1.61	1.70	1.58
metabolic process	0.91	0.92	0.98	1.10
endoplasmic reticulum	0.98	1.00	1.14	1.29
Golgi apparatus	1.07	1.05	1.04	1.06
neuromuscular process	1.24	1.50	0.82	0.95
autophagy	0.95	0.96	0.61	0.63

transducer action, an important process that helps muscle fibers to cope with mechanical stress.[37] Thus, our data confirm RCMH cells as a well-suited model for studying muscular pathologies of cytoskeleton in vitro, including consequences of mechanical stress burden. Different components of the extracellular matrix such as numerous identified collagen isoforms (COL4A3BP, COL1A1, COL1A2, COL2A1, COL4A1, COL4A2, COL5A1, COL5A2, COL6A1, COL6A2, COL6A3, COL8A1, COL17A1), integrins (ITGA2B, ITGA3, ITGA5, ITGA7, ITGAV, ITGB1, ITGB2, ITGB4, and ITGB5), integrin-related proteins (CIB1, ILK, ILKAP, and ITGB1P1), laminins (LAMA5, LAMB1 and 2, LAMC1), and assembly factors such as PGS1 (Supplemental Table 1) also provide physical stabilization during the extreme tensile forces generated by contraction and mechanical stress burden.[38,39] Hence, knowledge of the expression of these proteins in RCMH cells provides the basis for muscle in vitro experiments focusing on cytoskeleton and cytoskeleton-modifying mechanisms.

RCMH Proteome Composition Allows In vitro Investigation of the Dystroglycan Complex and Several Congenital Muscular Disorders

In mammalian muscle, dystrophin (DMD) connects cytoskeletal actin via the dystroglycan complex (DGC) to laminin (LAMB1) localized in the extracellular matrix. Thereby, β-dystroglycan, an integral plasma membrane protein, is non-covalently associated with α-dystroglycan and associated with a macromolecular protein complex: the α, β, γ, and δ-sarcoglycans (SGCA, SGCB, SGCG, SGCD), CAV3, SNTA1, SNTB1, dystrophin, DTNB, and the neuronal isoform of the nitric oxide synthase (NOS). The expression of DMD was already demonstrated by Caviedes and colleagues;[15] however, the number of DGC components expressed in RCMH cells is increased by our proteomic data: Apart from dystrophin, we identified dystroglycan (DAG1; expression highest in RCMH), SGCB (much higher in RCMH than in HeLa, not detected in U2OS), SGCD (only detected in RCMH), SNTA1 (RCMH much higher than HeLa, not detected in U2OS), SNTB1 (only detected in RCMH), SNTB2 (clearly highest expression in RCMH), and DTNB (considerably higher in RCMH than in HeLa, not detected in U2OS). Additionally, our proteomic map of RCMH cells includes NOS3 (not detected in HeLa nor U2OS), the endothelial isoform of the nitric oxide synthase as well as DGC assisting factors like ANK3 which are required for costamere localization of dystrophin and DAG1.[40] The value of RCMH cells as an in vitro model for myopathic processes is also highlighted by the detection of the DGC components previously mentioned and also by the expression of more than 90 myopathy-related proteins that are listed in Supplemental Table 1 (column N, involvement in disease).

RCMH Proteome Composition As a Prerequisite of In vitro Investigation on Muscle Metabolism

Muscle cells metabolize large amounts of glucose and fatty acids to fuel contraction and the marked concomitant ATP requirement.[41] The term metabolic myopathy is applied to a

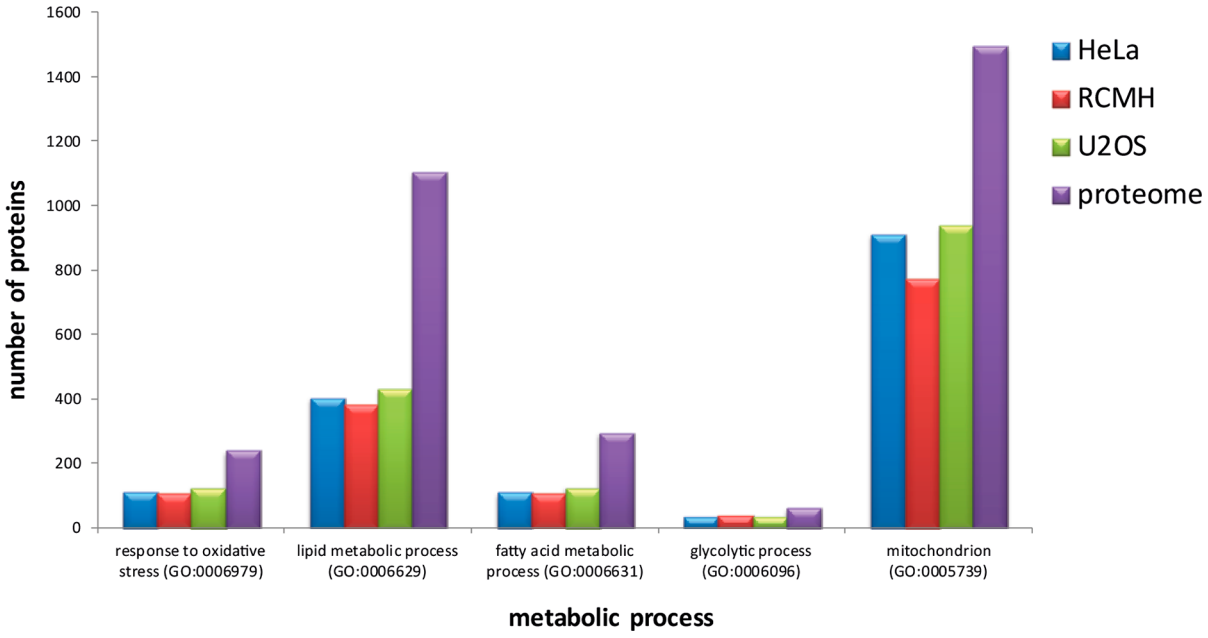

Figure 4. GO-term-based comparison of expression of proteins belonging to different metabolic areas in RCMH, HeLa, and U2OS and the Uniprot database ("proteome"; downloaded on 11th of December 2013, containing 20 273 target sequences).

DOI: 10.1021/acs.jproteome.5b00972
J. Proteome Res. 2016, 15, 945−955

heterogeneous group of diseases that result from the inability of the muscle cells to produce or retain adequate levels of ATP. Thereby, the metabolic myopathies can be categorized into muscle diseases due to (i) altered glycolytic activity/muscle glycogenosis, (ii) impaired lipid metabolism, (iii) impaired fatty acid metabolism, (iv) presence of oxidative stress, and (v) mitochondrial dysfunction.[42−45] Expression of proteins involved in the various aspects of metabolism is illustrated in Figure 4. Lipid metabolism represents the major source of energy for muscle fibers during prolonged exercise and symptoms associated with disorders of lipid metabolism typically appear after exercise. In this context, it is interesting to note that RCMH cells express proteins involved in neuromuscular lipid metabolism disorders (ABHD5, APOB, NSDHL; expression levels are similar in the three cell lines).

Muscle cells are characterized by a huge consumption of ATP and mitochondria function as cellular "power plants". Accordingly, mitochondrial dysfunction or damage can severely perturb metabolism, leading to muscular disorders.[46] Therefore, the known expression of the succinate dehydrogenase subunits SDHA, SDHB, SDHC, and of SDHAF2 as well as of the cytochrome *c* oxidase subunits COA3, COX5A, COX6B1, COX6C, COX7A2L, COX17, and TACO1 in RCMH provides a catalogue for in vitro studies of mitochondrial pathophysiology in muscular disorders. Hence, our proteome profile suggests that RCMH cells are a well-suited model for investigations on metabolic processes in muscle.

The pathophysiological impact of oxidative stress has been proposed to play a role in several types of muscular dystrophy (MD), collagen-, selenoprotein N-, and dysferlin-related myopathies, as well as the processes of muscle fatigue and injury. These results imply that oxidative stress, commonly connected to mitochondrial dysfunction, is detrimental for the homeostasis of muscle cells. Moreover, ryanodine receptor (RYR), a calcium channel and redox sensor, plays a role in muscle function during oxidative stress.[47−50] In this context, expression of not only this receptor (RYR3) but also different oxidoreductases such as ETFD, FDXR, FOXRED1, GLYR1, HTATIP2, NDUFS1, SQRDL, and WWOX as well as the nitric oxide synthase NOS3 in RCMH cells is worth noting. An increase in the expression of the redox-sensitive transcription factor NF-κB (NFKB1 and 2) leading to p65 (RELA) signaling-induced activation of the ubiquitin pathway is shown to occur in several muscle wasting disorders.[50] Expression of NF-κB, p65 and related proteins as well as of several proteins involved in the ubiquitin pathway (see Supplemental Table 1, Figure 1) is of particular interest with regard to the usability of RCMH myoblasts for investigating these pathways. The expression of these proteins is also interesting with respect to the in vitro study of neuromuscular disorders caused by extensive protein aggregation and/or proteolytic impairment (see below).

RCMH Proteome Composition Allows In vitro Investigation of SR/ER-Related Pathophysiology in Muscular Disorders

The sarcoendoplasmic reticulum (SR/ER), a major subcellular compartment of muscle fibers, plays a pivotal role in vital functions including translation and folding of membrane proteins and proteins of the secretory pathway as well as in calcium storage.[51,52] Calcium is sequestered in the SR and released after stimulation of the muscle cell, thus playing a major role in excitation-contraction coupling (see above). Moreover, the SR/ER is involved in cellular stress defense mechanisms like unfolded protein response (UPR) and ER-associated degradation pathway (ERAD).[53] Because disturbances in the protein processing capacity of the SR/ER are frequently associated with the manifestation of neuromuscular disorders,[52] the considerable expression of proteins belonging to these defense mechanisms (i.e., UPR- and ERAD-assisting factors like ATF6, BiP/HSPA5, CALR, CANX, DNAJB6, EDEM2 and 3, EIF2AK3/PERK, ERN1/IRE1, HSPA1A, HYOU1/GRP-170, P4HB/PDI, SIL1/BAP, and UGGT; Supplemental Table 1) suggests that RCMH cells can be used to investigate such pathophysiological processes. Notably, the three major transducers of UPR named ATF6, IRE1, and PERK were identified in RCMH, whereby IRE1 and PERK presented with much higher levels compared with HeLa or U2OS (Table 1). Several of these factors are involved in neuromuscular diseases (Supplemental Table 1). Moreover, expression of HSP90B1/GRP94/endoplasmin is also of particular interest for potential in vitro studies: GRP94 regulates insulin-like growth factor secretion in muscle cells and therefore has an important role in muscle differentiation and homeostasis, especially due to the production of contractile proteins.[54]

Several distinct domains with diverse functions comprise the ER.[55] One of these special domains is the nuclear envelope (NE), which is in continuity with the rough ER.[56] Notably, mutation of several nuclear envelope proteins leads to neuromuscular disorders. Well known examples are AAAS (aladin), EMD, LMNB1, ROGDI, SYNE1, and SYNE2, for which an expression could be demonstrated in RCMH. Similarly, the BiP-GRP170-SIL1 chaperone complex (cellular molecular ratio in RCMH ∼ 1:0.1:0.01) is expressed in RCMH cells. Localization of BiP within the NE of skeletal muscle fibers was already described in 1993,[57] and disturbances of this functional complex lead to Marinesco−Sjögren syndrome (MSS; MIM:248800), which is associated with specific NE alterations in the muscle biopsy of man and mouse.[58−60] A comparison of the BiP-GRP170-SIL1 molecular ratio in RCMH cells with the ratio in canine pancreas (∼1:0.1:0.001)[61] revealed increased SIL1 level in myoblastic cells, indicating a particular function of SIL1 in muscle tissue.

RCMH Proteome Allows Investigation of Ca^{2+}-Dependent Excitation-Contraction-Coupling-Related Proteins

Excitation−contraction coupling (EC coupling) is a fundamental process of muscle physiology, whereby the electrical stimulus is converted into a mechanical response (contraction). In skeletal muscle, this process relies on a direct coupling between the ryanodine receptor (RYR), a sarcoplasmic reticulum (SR) Ca^{2+} release channel, and dihydropyridine receptors (DHPRs), acting as voltage-gated L-type Ca^{2+}channels. DHPRs are located on the sarcolemma, which includes the surface sarcolemma and the transverse tubules. Thereby an action potential arrives to depolarize the sarcolemma/cell membrane, resulting in an increase in cytosolic Ca^{2+} (calcium transient), which in turn activates Ca^{2+}-sensitive contractile proteins. In RCMH cells, expression of RYR and DHPR/QDPR was already reported.[15,16,18] Consistent with this, we found expression of further contraction-related Ca^{2+}-dependent proteins such as ATP2A2, ATP2B1, ATP2B4, CACNA1S, ESYT1, ESYT2, KCNMA1, CAMK2D, CAMK2G, and CHERP (Supplemental Table 1). Apart from that, CALM1, CALU, and STIM1 were detected (Supplemental Table 1). Notably, accumulation of the latter proteins was linked to muscle fiber degeneration in neurogenic muscular

DOI: 10.1021/acs.jproteome.5b00972
J. Proteome Res. 2016, 15, 945−955

atrophies, in which EC coupling is altered due to neuronal dysfunction.[62] Moreover, the identified α and β chains of spectrin (SPTAN1, SPTBN1) (Supplemental Table 1) interact with CALM in a Ca^{2+}-dependent manner and are thus candidates for the Ca^{2+}-dependent movement of the cytoskeleton at the membrane, a process important for muscle contraction.[63,64] Therefore, our proteomic profile indicates that RCMH cells are suitable to study alterations in EC-coupling-related proteins upon change of physiological conditions.

Morphological Characteristics of RCMH Cells

The implementation of mammalian cells for clinical research or application often requires a synchronized, phenotypically homogeneous and well-described cell population. In this work, we defined the morphological characteristics of RCMH cells grown for 24 h, with the help of transmission (TEM) and scanning (SEM) electron microscopy. The latter investigation revealed spread cells that displayed cytoplasmic extensions. This is in contrast with the morphological characteristics of murine C_2C_{12} myoblastic cells for which a less villous or rather smoother surface is described.[65] However, these microscopic protrusions of the plasma membrane not only increase the cell surface but also are responsible for cellular communication and mechanotransduction. With respect to the latter function, it is important to note that mechanical signals and their proper reprocessing are critical for the development and maintenance of skeletal muscle.[66] Because the respective mechanisms that convert the influence of cell shape to biochemical alterations are often not fully understood,[67] this cell surface property defines RCMH cells as a well-suited model for studying relative processes on both the morphological and the biochemical level. Our TEM studies confirmed the presence of cytoplasmic extensions and moreover revealed prominent ribosome dense sarcoendoplasmic reticulum (ER) networks. This morphological finding is in line with an increased expression of ER proteins in RCMH cells as compared with U2OS (see Table 2), mirrored by the relative expression of 7.1% of SR/ER proteins including the major transducers (ATF6, PERK, IRE1) of the unfolded protein response (see Table 1 and Supplemental Table 1). On a more general note this finding indicates that RCMH cells are an appropriate model to study ER-related pathophysiological processes of muscle cells. Additionally, accumulations of cytoskeletal components/intermediate filaments are in line with our proteomic findings and suggest that RCMH cells are also suitable for in vitro studies of the cytoskeleton in muscle function.

Under appropriate cell culture conditions, RCMH cells can undergo fusion and myotube formation in vitro.[15] This also classifies RCMH cells as a promising model to study pathophysiological phenomena depending on the differentiation stage, such as Miyoshi muscular dystrophy 1 (MMD1; MIM:254130) and Limb Girdle Muscular Dystrophy type 2B (LGMD2B; MIM: 253601), both related to mutations in dysferlin.

CONCLUSIONS

In the present study, we aimed at characterizing the human myoblastic RCMH cell line on both the morphological and biochemical levels. Therefore, electron microscopic and proteomics studies were performed. Our results demonstrate that this cell line has a prominent rough endoplasmic reticulum and accumulations of cytoskeletal components/intermediate filaments and constitutively expresses proteins, leading to myoblastic differentiation as well as contractile and cytoskeletal proteins and shows an expression pattern of plasma membrane proteins and of proteins involved in muscular disorders. Our results demonstrate that this cell line is suitable for the investigation of relative processes like mechanical stress burden and mechanotransduction as well as ER-associated myopathic disorders.

ASSOCIATED CONTENT

Supporting Information

The Supporting Information is available free of charge on the ACS Publications website at DOI: 10.1021/acs.jproteome.5b00972.

Supplemental Table 1: Catalogue of proteins identified in RCMH cells along with information concerning their NSAF, molecular weight, subcellular localization, and involvement in diseases. (XLSX)

AUTHOR INFORMATION

Corresponding Author

*Tel: ++49-231-13924232. Fax: ++49-231-13924850. E-mail: andreas.roos@isas.de.

Author Contributions

The manuscript was written through contributions of all authors. All authors have given approval to the final version of the manuscript.

Notes

The authors declare no competing financial interest. Pablo Caviedes declares IP protection for the RCMH cell line.

ACKNOWLEDGMENTS

The financial support by the Ministerium für Innovation, Wissenschaft und Forschung des Landes Nordrhein-Westfalen and by the German Research Foundation (DFG ZA 639/1-1) is gratefully acknowledged. Additionally, this work has been supported by Rings grant ACT 1121 (Chile), by a grant from START program of RWTH Aachen University (to A.R.; grant no. 41/12), and by the Else Kröner-Fresenius Stiftung (to A.R.; grant no. A59/09).

ABBREVIATIONS

ACN, acetonitrile; BCA, bicinchoninic acid; GuHCl, guanidine hydrochloride; HeLa, human cervical cancer cell line; LC−MS/MS, liquid chromatography−andem mass spectrometry; TFA, trifluoroacetic acid; Tris, tris(hydroxymethyl)aminomethane; U2OS, human osteosarcoma cell line

REFERENCES

(1) Wang-Su, S. T.; McCormack, A. L.; Yang, S.; Hosler, M. R.; Mixon, A.; Riviere, M. A.; Wilmarth, P. A.; Andley, U. P.; Garland, D.; Li, H.; David, L. L.; Wagner, B. J. Proteome analysis of lens epithelia, fibers, and the HLE B-3 cell line. *Invest. Ophthalmol. Visual Sci.* **2003**, *44* (11), 4829−36.

(2) Riederer, I.; Negroni, E.; Bencze, M.; Wolff, A.; Aamiri, A.; Di Santo, J. P.; Silva-Barbosa, S. D.; Butler-Browne, G.; Savino, W.; Mouly, V. Slowing down differentiation of engrafted human myoblasts into immunodeficient mice correlates with increased proliferation and migration. *Mol. Ther.* **2012**, *20* (1), 146−54.

(3) Tannu, N. S.; Rao, V. K.; Chaudhary, R. M.; Giorgianni, F.; Saeed, A. E.; Gao, Y.; Raghow, R. Comparative proteomes of the proliferating C(2)C(12) myoblasts and fully differentiated myotubes

DOI: 10.1021/acs.jproteome.5b00972
J. Proteome Res. 2016, 15, 945−955

reveal the complexity of the skeletal muscle differentiation program. *Mol. Cell. Proteomics* **2004**, *3* (11), 1065−82.
(4) Kislinger, T.; Gramolini, A. O.; Pan, Y.; Rahman, K.; MacLennan, D. H.; Emili, A. Proteome dynamics during C2C12 myoblast differentiation. *Mol. Cell. Proteomics* **2005**, *4* (7), 887−901.
(5) Casadei, L.; Vallorani, L.; Gioacchini, A. M.; Guescini, M.; Burattini, S.; D'Emilio, A.; Biagiotti, L.; Falcieri, E.; Stocchi, V. Proteomics-based investigation in C2C12 myoblast differentiation. *Eur. J. Histochem.* **2009**, *53* (4), e31.
(6) Grossi, A.; Lametsch, R.; Karlsson, A. H.; Lawson, M. A. Mechanical stimuli on C2C12 myoblasts affect myoblast differentiation, focal adhesion kinase phosphorylation and galectin-1 expression: a proteomic approach. *Cell Biol. Int.* **2011**, *35* (6), 579−86.
(7) Forterre, A.; Jalabert, A.; Berger, E.; Baudet, M.; Chikh, K.; Errazuriz, E.; De Larichaudy, J.; Chanon, S.; Weiss-Gayet, M.; Hesse, A. M.; Record, M.; Geloen, A.; Lefai, E.; Vidal, H.; Coute, Y.; Rome, S. Proteomic analysis of C2C12 myoblast and myotube exosome-like vesicles: a new paradigm for myoblast-myotube cross talk? *PLoS One* **2014**, *9* (1), e84153.
(8) Kaufman, S. J.; Foster, R. F. Replicating myoblasts express a muscle-specific phenotype. *Proc. Natl. Acad. Sci. U. S. A.* **1988**, *85* (24), 9606−10.
(9) Partridge, T. A.; Morgan, J. E.; Coulton, G. R.; Hoffman, E. P.; Kunkel, L. M. Conversion of mdx myofibres from dystrophin-negative to -positive by injection of normal myoblasts. *Nature* **1989**, *337* (6203), 176−9.
(10) Deshmukh, A. S.; Murgia, M.; Nagaraj, N.; Treebak, J. T.; Cox, J.; Mann, M. Deep proteomics of mouse skeletal muscle enables quantitation of protein isoforms, metabolic pathways and transcription factors. *Mol. Cell. Proteomics* **2015**, *14*, 841.
(11) Stadler, G.; Chen, J. C.; Wagner, K.; Robin, J. D.; Shay, J. W.; Emerson, C. P., Jr.; Wright, W. E. Establishment of clonal myogenic cell lines from severely affected dystrophic muscles - CDK4 maintains the myogenic population. *Skeletal Muscle* **2011**, *1* (1), 12.
(12) Mamchaoui, K.; Trollet, C.; Bigot, A.; Negroni, E.; Chaouch, S.; Wolff, A.; Kandalla, P. K.; Marie, S.; Di Santo, J.; St Guily, J. L.; Muntoni, F.; Kim, J.; Philippi, S.; Spuler, S.; Levy, N.; Blumen, S. C.; Voit, T.; Wright, W. E.; Aamiri, A.; Butler-Browne, G.; Mouly, V. Immortalized pathological human myoblasts: towards a universal tool for the study of neuromuscular disorders. *Skeletal Muscle* **2011**, *1*, 34.
(13) Le Bihan, M. C.; Bigot, A.; Jensen, S. S.; Dennis, J. L.; Rogowska-Wrzesinska, A.; Laine, J.; Gache, V.; Furling, D.; Jensen, O. N.; Voit, T.; Mouly, V.; Coulton, G. R.; Butler-Browne, G. In-depth analysis of the secretome identifies three major independent secretory pathways in differentiating human myoblasts. *J. Proteomics* **2012**, *77*, 344−56.
(14) Robin, J. D.; Wright, W. E.; Zou, Y.; Cossette, S. C.; Lawlor, M. W.; Gussoni, E. Isolation and immortalization of patient-derived cell lines from muscle biopsy for disease modeling. *J. Visualized Exp.* **2015**, No. 95, 52307.
(15) Caviedes, R.; Liberona, J. L.; Hidalgo, J.; Tascon, S.; Salas, K.; Jaimovich, E. A human skeletal muscle cell line obtained from an adult donor. *Biochim. Biophys. Acta, Mol. Cell Res.* **1992**, *1134* (3), 247−55.
(16) Liberona, J. L.; Caviedes, P.; Tascon, S.; Hidalgo, J.; Giglio, J. R.; Sampaio, S. V.; Caviedes, R.; Jaimovich, E. Expression of ion channels during differentiation of a human skeletal muscle cell line. *J. Muscle Res. Cell Motil.* **1997**, *18* (5), 587−98.
(17) Carrasco, M. A.; Marambio, P.; Jaimovich, E. Changes in IP3 metabolism during skeletal muscle development in vivo and in vitro. *Comp. Biochem. Physiol., Part B: Biochem. Mol. Biol.* **1997**, *116* (2), 173−81.
(18) Liberona, J. L.; Powell, J. A.; Shenoi, S.; Petherbridge, L.; Caviedes, R.; Jaimovich, E. Differences in both inositol 1,4,5-trisphosphate mass and inositol 1,4,5-trisphosphate receptors between normal and dystrophic skeletal muscle cell lines. *Muscle Nerve* **1998**, *21* (7), 902−9.
(19) Burkhart, J. M.; Gambaryan, S.; Watson, S. P.; Jurk, K.; Walter, U.; Sickmann, A.; Heemskerk, J. W.; Zahedi, R. P. What can proteomics tell us about platelets? *Circ. Res.* **2014**, *114* (7), 1204−19.
(20) Prause, J.; Goswami, A.; Katona, I.; Roos, A.; Schnizler, M.; Bushuven, E.; Dreier, A.; Buchkremer, S.; Johann, S.; Beyer, C.; Deschauer, M.; Troost, D.; Weis, J. Altered localization, abnormal modification and loss of function of Sigma receptor-1 in amyotrophic lateral sclerosis. *Hum. Mol. Genet.* **2013**, *22* (8), 1581−600.
(21) Manza, L. L.; Stamer, S. L.; Ham, A.-J. L.; Codreanu, S. G.; Liebler, D. C. Sample preparation and digestion for proteomic analyses using spin filters. *Proteomics* **2005**, *5* (7), 1742−1745.
(22) Wisniewski, J. R.; Zougman, A.; Nagaraj, N.; Mann, M. Universal sample preparation method for proteome analysis. *Nat. Methods* **2009**, *6* (5), 359−362.
(23) Burkhart, J. M.; Schumbrutzki, C.; Wortelkamp, S.; Sickmann, A.; Zahedi, R. P. Systematic and quantitative comparison of digest efficiency and specificity reveals the impact of trypsin quality on MS-based proteomics. *J. Proteomics* **2012**, *75* (4), 1454−1462.
(24) Olsen, J. V.; de Godoy, L. M. F.; Li, G.; Macek, B.; Mortensen, P.; Pesch, R.; Makarov, A.; Lange, O.; Horning, S.; Mann, M. Parts per Million Mass Accuracy on an Orbitrap Mass Spectrometer via Lock Mass Injection into a C-trap. *Mol. Cell. Proteomics* **2005**, *4* (12), 2010−2021.
(25) Chambers, M. C.; Maclean, B.; Burke, R.; Amodei, D.; Ruderman, D. L.; Neumann, S.; Gatto, L.; Fischer, B.; Pratt, B.; Egertson, J.; Hoff, K.; Kessner, D.; Tasman, N.; Shulman, N.; Frewen, B.; Baker, T. A.; Brusniak, M. Y.; Paulse, C.; Creasy, D.; Flashner, L.; Kani, K.; Moulding, C.; Seymour, S. L.; Nuwaysir, L. M.; Lefebvre, B.; Kuhlmann, F.; Roark, J.; Rainer, P.; Detlev, S.; Hemenway, T.; Huhmer, A.; Langridge, J.; Connolly, B.; Chadick, T.; Holly, K.; Eckels, J.; Deutsch, E. W.; Moritz, R. L.; Katz, J. E.; Agus, D. B.; MacCoss, M.; Tabb, D. L.; Mallick, P. A cross-platform toolkit for mass spectrometry and proteomics. *Nat. Biotechnol.* **2012**, *30* (10), 918−20.
(26) Kim, S.; Gupta, N.; Pevzner, P. A. Spectral Probabilities and Generating Functions of Tandem Mass Spectra: A Strike against Decoy Databases. *J. Proteome Res.* **2008**, *7* (8), 3354−3363.
(27) Kim, S.; Mischerikow, N.; Bandeira, N.; Navarro, J. D.; Wich, L.; Mohammed, S.; Heck, A. J. R.; Pevzner, P. A. The Generating Function of CID, ETD, and CID/ETD Pairs of Tandem Mass Spectra: Applications to Database Search. *Mol. Cell. Proteomics* **2010**, *9* (12), 2840−2852.
(28) Vaudel, M.; Barsnes, H.; Berven, F. S.; Sickmann, A.; Martens, L. SearchGUI: An open-source graphical user interface for simultaneous OMSSA and X!Tandem searches. *Proteomics* **2011**, *11* (5), 996−999.
(29) Vaudel, M.; Burkhart, J. M.; Zahedi, R. P.; Oveland, E.; Berven, F. S.; Sickmann, A.; Martens, L.; Barsnes, H. PeptideShaker enables reanalysis of MS-derived proteomics data sets. *Nat. Biotechnol.* **2015**, *33* (1), 22−4.
(30) Zybailov, B.; Mosley, A. L.; Sardiu, M. E.; Coleman, M. K.; Florens, L.; Washburn, M. P. Statistical Analysis of Membrane Proteome Expression Changes in Saccharomyces cerevisiae. *J. Proteome Res.* **2006**, *5* (9), 2339−2347.
(31) Vizcaino, J. A.; Deutsch, E. W.; Wang, R.; Csordas, A.; Reisinger, F.; Rios, D.; Dianes, J. A.; Sun, Z.; Farrah, T.; Bandeira, N.; Binz, P.-A.; Xenarios, I.; Eisenacher, M.; Mayer, G.; Gatto, L.; Campos, A.; Chalkley, R. J.; Kraus, H.-J.; Albar, J. P.; Martinez-Bartolome, S.; Apweiler, R.; Omenn, G. S.; Martens, L.; Jones, A. R.; Hermjakob, H. ProteomeXchange provides globally coordinated proteomics data submission and dissemination. *Nat. Biotechnol.* **2014**, *32* (3), 223−226.
(32) Karpati, G.; Pouliot, Y.; Zubrzycka-Gaarn, E.; Carpenter, S.; Ray, P. N.; Worton, R. G.; Holland, P. Dystrophin is expressed in mdx skeletal muscle fibers after normal myoblast implantation. *Am. J. Pathol.* **1989**, *135* (1), 27−32.
(33) Giorgianni, F.; Desiderio, D. M.; Beranova-Giorgianni, S. Proteome analysis using isoelectric focusing in immobilized pH gradient gels followed by mass spectrometry. *Electrophoresis* **2003**, *24* (1−2), 253−9.
(34) Juretic, N.; Jorquera, G.; Caviedes, P.; Jaimovich, E.; Riveros, N. Electrical stimulation induces calcium-dependent up-regulation of

DOI: 10.1021/acs.jproteome.5b00972
J. Proteome Res. 2016, 15, 945−955

neuregulin-1beta in dystrophic skeletal muscle cell lines. *Cell. Physiol. Biochem.* **2012**, *29* (5−6), 919−30.
(35) Guo, X.; Trudgian, D. C.; Lemoff, A.; Yadavalli, S.; Mirzaei, H. Confetti: a multiprotease map of the HeLa proteome for comprehensive proteomics. *Mol. Cell. Proteomics* **2014**, *13* (6), 1573−84.
(36) Beck, M.; Schmidt, A.; Malmstroem, J.; Claassen, M.; Ori, A.; Szymborska, A.; Herzog, F.; Rinner, O.; Ellenberg, J.; Aebersold, R. The quantitative proteome of a human cell line. *Mol. Syst. Biol.* **2011**, *7*, 549.
(37) Jaalouk, D. E.; Lammerding, J. Mechanotransduction gone awry. *Nat. Rev. Mol. Cell Biol.* **2009**, *10* (1), 63−73.
(38) Kjaer, M. Role of extracellular matrix in adaptation of tendon and skeletal muscle to mechanical loading. *Physiol. Rev.* **2004**, *84* (2), 649−98.
(39) Kaariainen, M.; Liljamo, T.; Pelto-Huikko, M.; Heino, J.; Jarvinen, M.; Kalimo, H. Regulation of alpha7 integrin by mechanical stress during skeletal muscle regeneration. *Neuromuscular disorders: NMD* **2001**, *11* (4), 360−9.
(40) Devarajan, P.; Stabach, P. R.; Mann, A. S.; Ardito, T.; Kashgarian, M.; Morrow, J. S. Identification of a small cytoplasmic ankyrin (AnkG119) in the kidney and muscle that binds beta I sigma spectrin and associates with the Golgi apparatus. *J. Cell Biol.* **1996**, *133* (4), 819−30.
(41) Egan, B.; Zierath, J. R. Exercise metabolism and the molecular regulation of skeletal muscle adaptation. *Cell Metab.* **2013**, *17* (2), 162−84.
(42) van Adel, B. A.; Tarnopolsky, M. A. Metabolic myopathies: update 2009. *Journal of clinical neuromuscular disease* **2009**, *10* (3), 97−121.
(43) Comi, G. P.; Fortunato, F.; Lucchiari, S.; Bordoni, A.; Prelle, A.; Jann, S.; Keller, A.; Ciscato, P.; Galbiati, S.; Chiveri, L.; Torrente, Y.; Scarlato, G.; Bresolin, N. Beta-enolase deficiency, a new metabolic myopathy of distal glycolysis. *Ann. Neurol.* **2001**, *50* (2), 202−7.
(44) Massa, R.; Lodi, R.; Barbiroli, B.; Servidei, S.; Sancesario, G.; Manfredi, G.; Zaniol, P.; Bernardi, G. Partial block of glycolysis in late-onset phosphofructokinase deficiency myopathy. *Acta Neuropathol.* **1996**, *91* (3), 322−9.
(45) Tobon, A. Metabolic myopathies. *Continuum* **2013**, *19* (6 Muscle Disease), 1571−97.
(46) Russell, A. P.; Foletta, V. C.; Snow, R. J.; Wadley, G. D. Skeletal muscle mitochondria: a major player in exercise, health and disease. *Biochim. Biophys. Acta, Gen. Subj.* **2014**, *1840* (4), 1276−84.
(47) Sorato, E.; Menazza, S.; Zulian, A.; Sabatelli, P.; Gualandi, F.; Merlini, L.; Bonaldo, P.; Canton, M.; Bernardi, P.; Di Lisa, F. Monoamine oxidase inhibition prevents mitochondrial dysfunction and apoptosis in myoblasts from patients with collagen VI myopathies. *Free Radical Biol. Med.* **2014**, *75C*, 40−47.
(48) Pereira, Y. C.; Nascimento, G. C.; Iyomasa, D. M.; Iyomasa, M. M. Muscle characterization of reactive oxygen species in oral diseases. *Acta Odontol. Scand.* **2015**, *73*, 81−86.
(49) Arbogast, S.; Beuvin, M.; Fraysse, B.; Zhou, H.; Muntoni, F.; Ferreiro, A. Oxidative stress in SEPN1-related myopathy: from pathophysiology to treatment. *Ann. Neurol.* **2009**, *65* (6), 677−86.
(50) Rajakumar, D.; Senguttuvan, S.; Alexander, M.; Oommen, A. Involvement of oxidative stress, nuclear factor kappa B and the ubiquitin proteasomal pathway in dysferlinopathy. *Life Sci.* **2014**, *108* (1), 54−61.
(51) Glembotski, C. C. Roles for the sarco-/endoplasmic reticulum in cardiac myocyte contraction, protein synthesis, and protein quality control. *Physiology* **2012**, *27* (6), 343−50.
(52) Yang, W.; Paschen, W. The endoplasmic reticulum and neurological diseases. *Exp. Neurol.* **2009**, *219* (2), 376−81.
(53) Caspersen, C.; Pedersen, P. S.; Treiman, M. The sarco/endoplasmic reticulum calcium-ATPase 2b is an endoplasmic reticulum stress-inducible protein. *J. Biol. Chem.* **2000**, *275* (29), 22363−72.
(54) Ostrovsky, O.; Ahmed, N. T.; Argon, Y. The chaperone activity of GRP94 toward insulin-like growth factor II is necessary for the stress response to serum deprivation. *Molecular biology of the cell* **2009**, *20* (6), 1855−64.
(55) Lynes, E. M.; Simmen, T. Urban planning of the endoplasmic reticulum (ER): how diverse mechanisms segregate the many functions of the ER. *Biochim. Biophys. Acta, Mol. Cell Res.* **2011**, *1813* (10), 1893−905.
(56) Clever, M.; Mimura, Y.; Funakoshi, T.; Imamoto, N. Regulation and coordination of nuclear envelope and nuclear pore complex assembly. *Nucleus* **2013**, *4* (2), 105−14.
(57) Villa, A.; Podini, P.; Nori, A.; Panzeri, M. C.; Martini, A.; Meldolesi, J.; Volpe, P. The endoplasmic reticulum-sarcoplasmic reticulum connection. II. Postnatal differentiation of the sarcoplasmic reticulum in skeletal muscle fibers. *Exp. Cell Res.* **1993**, *209* (1), 140−8.
(58) Senderek, J.; Krieger, M.; Stendel, C.; Bergmann, C.; Moser, M.; Breitbach-Faller, N.; Rudnik-Schoneborn, S.; Blaschek, A.; Wolf, N. I.; Harting, I.; North, K.; Smith, J.; Muntoni, F.; Brockington, M.; Quijano-Roy, S.; Renault, F.; Herrmann, R.; Hendershot, L. M.; Schroder, J. M.; Lochmuller, H.; Topaloglu, H.; Voit, T.; Weis, J.; Ebinger, F.; Zerres, K. Mutations in SIL1 cause Marinesco-Sjogren syndrome, a cerebellar ataxia with cataract and myopathy. *Nat. Genet.* **2005**, *37* (12), 1312−4.
(59) Krieger, M.; Roos, A.; Stendel, C.; Claeys, K. G.; Sonmez, F. M.; Baudis, M.; Bauer, P.; Bornemann, A.; de Goede, C.; Dufke, A.; Finkel, R. S.; Goebel, H. H.; Haussler, M.; Kingston, H.; Kirschner, J.; Medne, L.; Muschke, P.; Rivier, F.; Rudnik-Schoneborn, S.; Spengler, S.; Inzana, F.; Stanzial, F.; Benedicenti, F.; Synofzik, M.; Lia Taratuto, A.; Pirra, L.; Tay, S. K.; Topaloglu, H.; Uyanik, G.; Wand, D.; Williams, D.; Zerres, K.; Weis, J.; Senderek, J. SIL1 mutations and clinical spectrum in patients with Marinesco-Sjogren syndrome. *Brain* **2013**, *136* (Pt 12), 3634−44.
(60) Roos, A.; Buchkremer, S.; Kollipara, L.; Labisch, T.; Gatz, C.; Zitzelsberger, M.; Brauers, E.; Nolte, K.; Schroder, J. M.; Kirschner, J.; Jesse, C. M.; Goebel, H. H.; Goswami, A.; Zimmermann, R.; Zahedi, R. P.; Senderek, J.; Weis, J. Myopathy in Marinesco-Sjogren syndrome links endoplasmic reticulum chaperone dysfunction to nuclear envelope pathology. *Acta Neuropathol.* **2014**, *127* (5), 761−77.
(61) Zahedi, R. P.; Volzing, C.; Schmitt, A.; Frien, M.; Jung, M.; Dudek, J.; Wortelkamp, S.; Sickmann, A.; Zimmermann, R. Analysis of the membrane proteome of canine pancreatic rough microsomes identifies a novel Hsp40, termed ERj7. *Proteomics* **2009**, *9* (13), 3463−73.
(62) Goswami, A.; Jesse, C.; Chandrasekar, A.; Bushuven, E.; Vollrath, J.; Dreser, A.; Katona, I.; Beyer, C.; Johann, S.; Feller, A.; Grond, M.; Wagner, S.; Nikolin, S.; Troost, D.; Weis, J. Accumulation of STIM1 is associated with the degenerative muscle fibre phenotype in ALS and other neurogenic atrophies. *Neuropathol. Appl. Neurobiol.* **2015**, *41* (3), 304−318.
(63) Gautel, M. Cytoskeletal protein kinases: titin and its relations in mechanosensing. *Pfluegers Arch.* **2011**, *462* (1), 119−34.
(64) Psatha, M. I.; Razi, M.; Koffer, A.; Moss, S. E.; Sacks, D. B.; Bolsover, S. R. Targeting of calcium:calmodulin signals to the cytoskeleton by IQGAP1. *Cell Calcium* **2007**, *41* (6), 593−605.
(65) Muratore, M.; Mitchell, S.; Waterfall, M. Plasma membrane characterization, by scanning electron microscopy, of multipotent myoblasts-derived populations sorted using dielectrophoresis. *Biochem. Biophys. Res. Commun.* **2013**, *438* (4), 666−72.
(66) Benavides Damm, T.; Egli, M. Calcium's role in mechanotransduction during muscle development. *Cell. Physiol. Biochem.* **2014**, *33* (2), 249−72.
(67) Burkholder, T. J. Mechanotransduction in skeletal muscle. *Front. Biosci., Landmark Ed.* **2007**, *12*, 174−91.

DOI: 10.1021/acs.jproteome.5b00972
J. Proteome Res. 2016, 15, 945−955